Available online at www.sciencedirect.com
SCIENCE DIRECT®
PERGAMON
Polyhedron 22 (2003) 299–305
POLYHEDRON
www.elsevier.com/locate/poly

New ion-pair nickel(III) complexes containing [Ni('S_2')$_2$] ('S_2'$^{2-}$ = 1,2-benzenedithiolate) fragments: synthesis, crystal structure and properties

Jing-Li Xie [a], Xiao-Ming Ren [a,*], Cheng He [b], You Song [a], Chun-Yin Duan [a], Song Gao [b], Qing-Jin Meng [a,*]

[a] State Key Laboratory of Coordination Chemistry, Coordination Chemistry Institute, Nanjing University, 210093 Nanjing, People's Republic of China
[b] State Key Laboratory of Rare Earth Materials Chemistry and Applications, Peking University, 100871 Beijing, People's Republic of China

Received 4 July 2002; accepted 22 October 2002

Abstract

Two new ion-pair complexes [1-(4′-fluorobenzyl)pyridinium][Ni(bdt)$_2$] (**1**) and [1-(4′-bromobenzyl)pyridinium][Ni(bdt)$_2$] (**2**), in which bdt^{2-} = 1,2-benzenedithiolate ('S_2'$^{2-}$), have been prepared and characterized. X-ray structural analyses showed that **1** and **2** are isostructural, and the anions are centrosymmetric. The 2 non-equiv. anions form different uniform-spaced stacking pattern in **1** and **2**. The magnetic measurements of **1** and **2** indicate ferromagnetic behavior in the antiferromagnetic exchange system, which may arise from spin canting. Cyclovoltammetry revealed two quasi-reversible one-electron steps for **1** and **2**, which are attributed to Ni(IV/III) and Ni(III/II) redox couples.

Keywords: Ni(III) thiolate complexes; Crystal structures; Magnetism; Spin canting

1. Introduction

Recently, much attention has focused on the coordination chemistry of unsaturated chalcogen ligands due to their electrochemistry and photochemistry as well as their potential applications as non-linear optical materials [1,2]. Moreover, numerous complexes containing [M('S_2')$_2$] fragments ['S_2'$^{2-}$ = 1,2-benzenedithiolate] can bind and activate or stabilize a considerable number of small molecules that are key intermediates in enzymatic process [3] as well as model compounds for the active sites in nitrogenase or for certain nickel enzymes [4]. But the reports on ion-pair complexes containing [M('S_2')$_2$]$^{z-}$ ($z = 1$, or 2) are rare, and unambiguous structural determination of these complexes by X-ray diffraction is still lacking [5]. Up to now, few analogous complexes containing the planar [Ni($S_2C_6H_4$)$_2$]$^{n-}$ anions with $n = 2$ and 1 have been characterized by X-ray analysis [6]. Also, exploration of their magnetic properties is still very rare. We have recently developed a new class of ion-pair complexes [RBzPy]$^+$[Ni(mnt)$_2$]$^-$ ([RBzPy]$^+$ = benzylpyridinium derivative and mnt^{2-} = maleonitriledithiolate) and found that the molecular conformation of the [RBzPy]$^+$ cation, which is related to its topology and size, can be modified by systematic variation of the substituent groups in the aromatic rings. Furthermore, the crystal structure of those complexes could be influenced [7]. With the goal of extending further investigation of this class of bis(dithiolato) transition metal complexes, we have pursued the study of complexes consisting of planar [Ni('S_2')$_2$]$^-$ anion and substituted benzylpyridinium cation, and explore their structures and unexpected magnetic properties.

* Corresponding authors. Fax: +25-331-4502
E-mail addresses: njujlxie@yahoo.com (X.-M. Ren), mengqj@netra.nju.edu.cn (Q.-J. Meng).

0277-5387/02/$ - see front matter
PII: S0277-5387(02)01334-7

2. Experimental

2.1. Reagents and physical measurements

All chemicals and solvents were of reagent grade and were used without further purification. Benzene-1,2-dithiol was purchased from TCI chemicals, 1-(4′-fluorobenzyl)pyridinium chloride ([FBzPy]Cl) and 1-(4′-bromobenzyl)pyridinium bromide ([BrBzPy]Br) were prepared as described in the literature [8]. Elemental analyses were performed with a Perkin–Elmer 240 analytical instrument. A Bruker IFS66V FT IR spectrophotometer was used, and the measurements were made by the KBr disk method. ^{1}H NMR spectra were recorded on a Bruker AVANCE300 spectrometer in DMSO-d_6 solution at 20 °C. The ESR spectra were recorded on a Bruker ER200D-SRC spectrometer at 100 kHz modulation at room temperature. Mn^{2+} in MgO was used as the standard sample. Magnetic susceptibility data on powder-sample were measured over a temperature range of 2–300 K on a Model Maglab System^{2000} magnetometer. Diamagnetic corrections were made using Pascal's constants. Cyclic voltammograms were recorded on a EG&G potentiostat/galvanostat model 273 analyzer in a one-comportment cell (glassy carbon working electrode, Pt counter electrode and Ag–AgCl reference electrode) under an Ar atmosphere at 25 °C in MeCN solution with approximately 0.1 M $[Bu_4N]ClO_4$ as conducting electrolyte. In the −1.2 to +1.2 V region, a potential scan rate of 100 mV s^{-1} was used.

2.2. Preparations

2.2.1. Synthesis of [FBzPy][Ni(bdt)$_2$] (1)

Under nitrogen atmosphere at room temperature, benzene-1,2-dithiol (284 mg, 2 mmol) was added to a solution of sodium metal (92 mg, 4 mmol) in 25 ml of absolute ethanol. A solution of $NiCl_2\cdot 6H_2O$ (240 mg, 1 mmol) in ethanol was added, resulting in the formation of a muddy red–brown color. Following this, [FBzPy]Cl (244 mg, 2 mmol) was added and the mixture allowed to stand with stirring for 1 h, and then stirred for 24 h with the presence of atmosphere. The color of the mixture gradually turned green, indicating oxidation from a dianionic species to the more stable monoanionic form. The precipitate was washed with absolute ethanol and ether and then dried. The crude product was recrystallized twice from methylene chloride to give 368 mg dark green needles. Yield: 69%. *Anal*. Found: C, 54.8; H, 3.6; N, 2.6. Calc. for $C_{24}H_{19}FNNiS_4$: C, 54.7; H, 3.6; N, 2.7%. IR (cm^{-1}): 3033 (w), 2964 (s, ν(CH)), 2854 (m, ν(CH)), 1482 (vs, δ(CH)), 1419 (s), 1224 (m), 737, 666 (vs, ν(C–S)). ^{1}H NMR: δ 9.15 (2H, CHC(F)CH), 8.60(1H, ArH, pyridine ring), 8.16 (2H, CH(C)CH, phenyl ring), 7.61, 7.29 (4H, $C_6H_4S_2$), 5.93 (4H, $(CH)_2N(CH)_2$, pyridine ring), 2.63 (2H, CH_2N).

2.2.2. Synthesis of [BrBzPy][Ni(bdt)$_2$] (2)

[BrBzPy][Ni(bdt)$_2$] (**2**) was prepared by the same procedure. Yield: 72%. *Anal.* Found: C, 49.2; H, 3.3; N, 2.4. Calc. for $C_{24}H_{19}BrNNiS_4$: C, 49.0; H, 3.3; N, 2.4%. IR (cm^{-1}): 3035 (w), 2968 (s, ν(CH)), 2851 (m, ν(CH)), 1480 (vs, δ(CH)), 1411 (s), 737, 664 (vs, ν(C–S)). ^{1}H NMR: δ 9.14 (2H, CHC(F)CH), 8.62 (1H, ArH, pyridine ring), 8.16 (2H, CH(C)CH, phenyl ring), 7.67, 7.49 (4H, $C_6H_4S_2$), 5.82 (4H, $(CH)_2N(CH)_2$, pyridine ring), 2.63 (2H, CH_2N).

2.2.3. Crystal structure determination

Diffraction data of complexes **1** and **2** were collected at 293 K on a Siemens SMART CCD area detector equipped with graphite-monochromated Mo Kα radiation. Crystal data collection parameters and refinement details are listed in Table 1. All computations were carried out using the SHELXTL-PC program package [9]. The structure was solved by direct method and refined on F^2 by full-matrix least-squares methods. All the nonhydrogen atoms were refined anisotropically. Hydrogen atoms were placed in their calculated positions and refined following the riding model.

3. Results and discussions

3.1. Crystal structure

An ORTEP drawing with the atomic labeling of the molecular unit is shown in Fig. 1. Selected bond distances and bond angles are listed in Table 2. The molecular structure of **1** contains two different, independent halves of centrosymmetric $[Ni(bdt)_2]^-$ anions, and one $[FBzPy]^+$ cation.

The nickel atoms are each surrounded by four sulfur atoms in square-planar geometry, which is markedly different from a spiro compound $Si(bdt)_2$ [10]. As for the Ni(1)-containing unit, the Ni(1)–S(1) and Ni(1)–S(2) distances are 2.148 and 2.151 Å, respectively. The values are in agreement with the analogous $[Ni(bdt)_2]^-$ complex reported [6b]. The S–Ni–S bond angle within the five-member ring is 91.77(2)°, which is slightly larger than that observed in complex with substituent groups on benzene rings [6c]. There exists a dihedral angle of 2.6° between C(1)C(2)C(3)C(4)C(5)C(6)S(1)S(2) (abbr. C_6S_2) and the Ni(1)S(1)S(2) planes, so the anion adopts an envelope conformation, and the Ni(1) atom deviates 0.08 Å from C_6S_2 plane. In Ni(2)-containing unit, the Ni–S bonds cover the range from 2.14 to 2.16 Å and the S–Ni–S bond angle within the five-member ring is 91.29(3)° which is in agreement with that of Ni(1)-containing unit. The Ni(2) atom deviates 0.12 Å from C(7)C(8)C(9)C(10)C(11)C(12)S(3)S(4) plane and the angle between C_6S_2 and the Ni(2)S(3)S(4) planes is 4.4°. The Ni(1)C_6S_2 and Ni(2)C_6S_2 planes are nearly

Table 1
Crystal data and refinement parameters

Formula	$C_{24}H_{19}FNNiS_4$	$C_{24}H_{19}BrNNiS_4$
Formula weight	527.35	588.26
Wavelength (Å)	0.71073	0.71073
Crystal system	triclinic	triclinic
Space group	$P\bar{1}$	$P\bar{1}$
Crystal color	black	black
Crystal size (mm)	$0.22 \times 0.22 \times 0.07$	$0.25 \times 0.10 \times 0.10$
Unit cell dimensions		
a (Å)	11.6607(12)	12.141(2)
b (Å)	14.3069(14)	14.342(3)
c (Å)	7.0960(4)	7.0763(14)
α (°)	92.7867(15)	93.32(3)
β (°)	93.623(5)	96.07(3)
γ (°)	96.2389(18)	99.00(3)
V (Å^3)	1172.61(18)	1206.7(4)
Z	2	2
D_{calc} (Mg m^{-3})	1.494	1.619
Absorption coefficient (mm^{-1})	1.204	2.818
F(000)	542	594
θ Range (°)	1.43–27.48	3.42–25.00
Index ranges	$0 \le h \le 15$, $-18 \le k \le 18$, $-9 \le l \le 9$	$-14 \le h \le 14$, $-17 \le k \le 17$, $-8 \le l \le 8$
Reflections collected	5094	15 258
Independent reflections	5094 [$R_{int} = 0.0000$]	4232 [$R_{int} = 0.0327$]
Absorption correction	empirical	empirical
Max. and min. transmission	0.920 and 0.762	0.755 and 0.496
Refinement method	Full-matrix least-squares on F^2	
Data/restraints/parameters	5094/0/283	4232/0/283
Goodness-of-fit on F^2	1.008	1.027
Final R indices [$I > 2\sigma(I)$]	$R_1 = 0.0356$, $wR_2 = 0.0846$	$R_1 = 0.0421$, $wR_2 = 0.1019$
R indices (all data)	$R_1 = 0.0507$, $wR_2 = 0.0922$	$R_1 = 0.0536$, $wR_2 = 0.1063$
Largest difference peak and hole (e Å^{-3})	0.259 and −0.382	1.024 and −1.038

perpendicular to each other with the dihedral angle of 84.2°. In the 1-(4′-fluorobenzyl)pyridinium cation, the dihedral angles of the N(1)–C(18)–C(19) reference plane are 71.8° for phenyl ring, 52.9° for pyridine ring, respectively. The phenyl ring and the pyridine ring make a dihedral angle of 103.2°.

The molecule packing of two anion units in **1** is different from each other (Fig. 2). The Ni(1)-containing units stack in side by side fashion, in which the anions with uniform spaced arrangements to form one dimensional (1-D) chain along c-axis, and the shortest distance between adjacent Ni(III) ions is 7.096 Å. Conversely, the Ni(2)-containing units stack in face to face fashion with an alternating arrangement of $[Ni(bdt)_2]^-$ anion and $[FBzPy]^+$ cation such that the pyridine ring moiety of cation lie above the phenyl ring moiety of the corresponding Ni(2)-containing units and vice versa. The shortest distance between adjacent Ni(III) ions is 7.096 Å, too. Between the most adjacent Ni(1)-containing and Ni(2)-containing units, a Ni···Ni distance of 7.153 Å is found.

Complex **2** is isostructural with **1**, the average Ni–S, C–S bond distance and bond angle of S–Ni–S within the five-member ring in the 2 non-equiv. anions are in agreement with that of **1** (Table 3). The dihedral angles between Ni(1)S(1)S(2) and C(1)C(2)C(3)C(4)C(5)C(6)-S(1)S(2) (abbr. C_6S_2) planes, Ni(2)S(3)S(4) and corresponding C_6S_2 planes are 4.6°, 2.3°, respectively. Also, the Ni(1)C_6S_2 and Ni(2)C_6S_2 planes make a dihedral angle of 80.9°. As for the 1-(4′-bromobenzyl)pyridinium cation, the dihedral angles between the N(1)–C(18)–C(19) reference plane and the aryl rings are 59.1° of phenyl ring, 66.0° of pyridine ring, respectively. The phenyl ring and the pyridine ring make a dihedral angle of 101.1°. The stacking pattern of **2** is similar to that of **1**, since variation of the substituents in the *para*-position of a benzyl group would not be expected to affect the conformation of the $[RBzPy]^+$ cation in this series of complexes.

3.2. Magnetic properties

The temperature dependence of the magnetic susceptibility for the powdered sample of **1** was measured in the range of 2–300 K in the form of the $\chi_m T$ versus T curve, where χ_m is the molar magnetic susceptibility (Fig. 3). Its magnetic behavior may be divided into three parts on their temperature dependence. The value of $\chi_m T$ at 300 K is estimated at 0.370 emu K mol^{-1}, and is nearly equal to that of spin-only of one $S = 1/2$ spin per formula unit. The $\chi_m T$ values decrease continuously upon cooling until 173 K, indicating the presence of antiferromagnetic exchange between metal centers. Then, the $\chi_m T$ values increases gradually between 173 and 15 K and reaches a maximum at approximately 15 K ($\chi_m T = 0.356$ emu K mol^{-1}) exhibiting ferromagnetic coupling behavior. The magnetic behavior in the temperature range 300–15 K may arise from spin-canting mechanism. Spin canting arises through a Dzyaloshinsky–Moriya interaction, which minimizes the coupling energy when two spins are perpendicular to one another, and this magnitude is proportional to $\Delta g/g$. At room temperature complex **1** show powder ESR spectrum as depicted in top of Fig. 4, which shows considerable anisotropy of the g-tensor [11]. From this it can be inferred that $g_x = 2.142$, $g_y = 2.097$, $g_z = 2.042$. Furthermore, it should be fulfilled when canting spins in

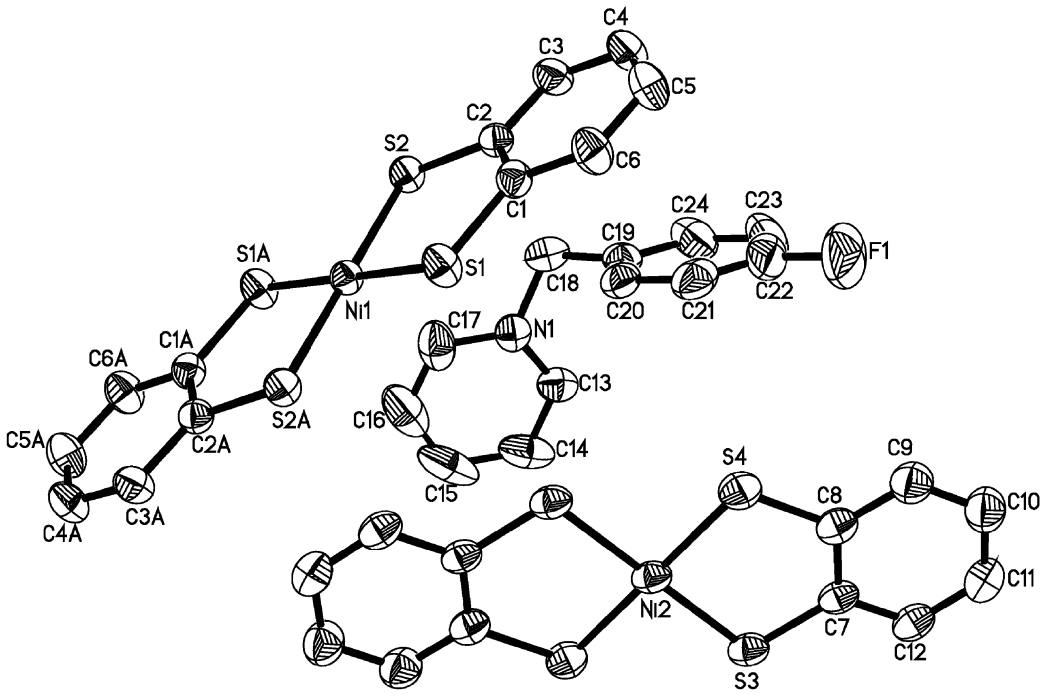

Fig. 1. ORTEP view with non-H atomic numbering scheme for **1**; 30% probability thermal ellipsoids are shown.

Table 2
Selected bond distances (Å) and angles (°) for **1** [a]

Bond distances			
Ni(1)–S(1)	2.1476(6)	Ni(1)–S(2)	2.1508(5)
Ni(2)–S(4)	2.1410(8)	Ni(2)–S(3)	2.1637(7)
S(1)–C(1)	1.741(2)	S(2)–C(2)	1.740(2)
S(3)–C(7)	1.736(3)	S(4)–C(8)	1.744(3)
C(1)–C(2)	1.395(3)	C(7)–C(8)	1.395(3)
Bond angles			
S(1)–Ni(1)–S(2)#1	88.23(2)	S(1)–Ni(1)–S(2)	91.77(2)
S(4)#2–Ni(2)–S(3)	88.71(3)	S(4)–Ni(2)–S(3)	91.29(3)
C(1)–S(1)–Ni(1)	105.10(8)	C(2)–S(2)–Ni(1)	104.98(7)

[a] Symmetry transformations used to generate equivalent atoms: #1 $-x, -y, -z$; #2 $-x, -y+1, -z$.

the solid state are not related by a center of inversion [12]. Based on its crystal structure, it is worth noting that the 2 non-equiv. Ni(III) ions do not relate to each other through an inversion center, and thus there may exist incomplete cancellation of spins between Ni(1)-containing and Ni(2)-containing units. When the temperature is below 15 K, the $\chi_m T$ values decrease quickly and drop to 0.275 emu K mol^{-1} at extremely low temperatures and this phenomenon may origin from magnetization saturation effect [13]. The data over the entire temperature are best fit by the Bonner–Fisher model for a uniformly spaced chain of $S = 1/2$ spin [14]. Eq. (1) for $H = -2JS_1S_2$ [15] with $z = J/k_BT$.

$$\chi_m = \frac{Ng^2\mu_B^2}{k_BT} \times \frac{0.25 + 0.074975z + 0.075235z^2}{1.0 + 0.9331z + 0.172135z^2 + 0.757825z^3} \quad (1)$$

A fit of the data to Eq. (1) gives $J = -11.5$ cm^{-1} and $g = 2.08$. So complex **1** behaves as a 1-D chain with appreciable antiferromagnetic interactions between the $S = 1/2$ Ni(III) spin carriers. As shown in Fig. 5, the field dependence of the magnetization (0–60 kOe) measured at 1.8 K shows the highest magnetization of approximately 98 emu G mol^{-1} is significantly smaller than the theoretical saturation value of 5585 emu G mol^{-1}, supporting the spin-canted structure for this complex [12a].

The magnetic behavior of **2** is similar to that of **1**, which also can be divided into three parts on their temperature dependence (Fig. 6). The value of $\chi_m T$ decreases with temperature to 230 K at which point there is a gradual increase to a maximum value before decreasing with decreasing temperature in the lowest temperature region. At temperatures above 230 K the compound shows antiferromagnetic exchange interaction between spin carriers (Ni(III) centers). Then the gradually increasing tendency between 230 and 11 K imply there exists ferromagnetic behavior and reaches a maximum at approximately 11 K ($\chi_m T = 0.388$ emu K mol^{-1}). When the temperature is below 11 K, the values of $\chi_m T$ decreasing with decreasing temperature. Fitting results from Bonner–Fisher model are $J = -11.7$ cm^{-1}

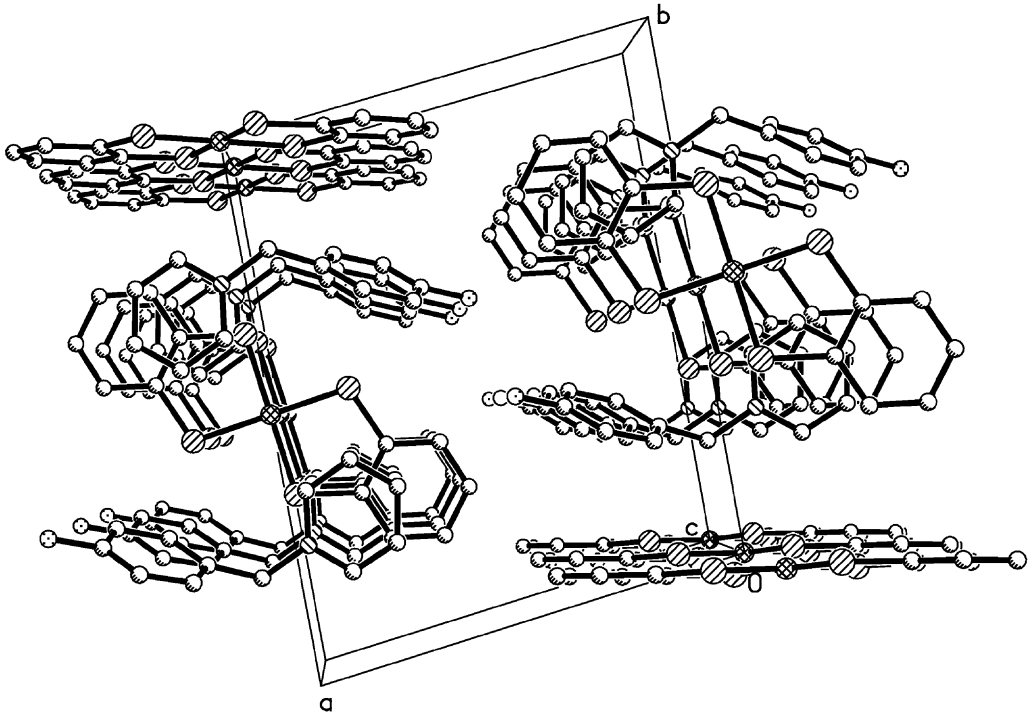

Fig. 2. The packing diagram of a unit cell for **1**.

Table 3
Selected bond lengths (Å) and angles (°) for **2** [a]

Bond distances			
Ni(1)–S(1)	2.1407(12)	Ni(1)–S(2)	2.1558(10)
Ni(2)–S(4)	2.1471(10)	Ni(2)–S(3)	2.1486(11)
S(1)–C(1)	1.744(4)	S(2)–C(2)	1.738(4)
S(3)–C(7)	1.740(3)	S(4)–C(8)	1.740(4)
C(1)–C(2)	1.392(5)	C(7)–C(8)	1.396(5)
Bond angles			
S(1)#1–Ni(1)–S(2)	88.41(5)	S(1)–Ni(1)–S(2)	91.59(5)
S(4)–Ni(2)–S(3)#2	88.23(4)	S(4)–Ni(2)–S(3)	91.77(4)
C(1)–S(1)–Ni(1)	105.23(14)	C(2)–S(2)–Ni(1)	105.01(13)

[a] Symmetry transformations used to generate equivalent atoms: #1 $-x, -y, -z+1$; #2 $-x+2, -y+1, -z+1$.

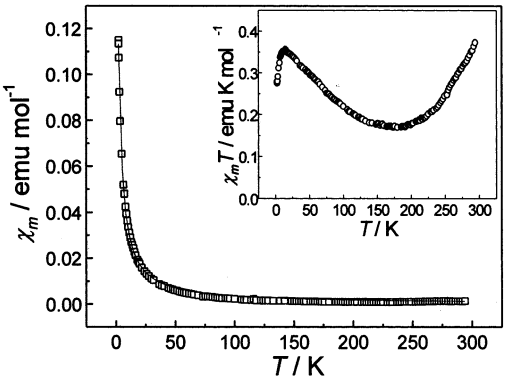

Fig. 3. Variation of molar magnetic susceptibility χ_m of **1** as a function of temperature. The solid line represents the best fit (inset: $\chi_m T$ vs. T plot).

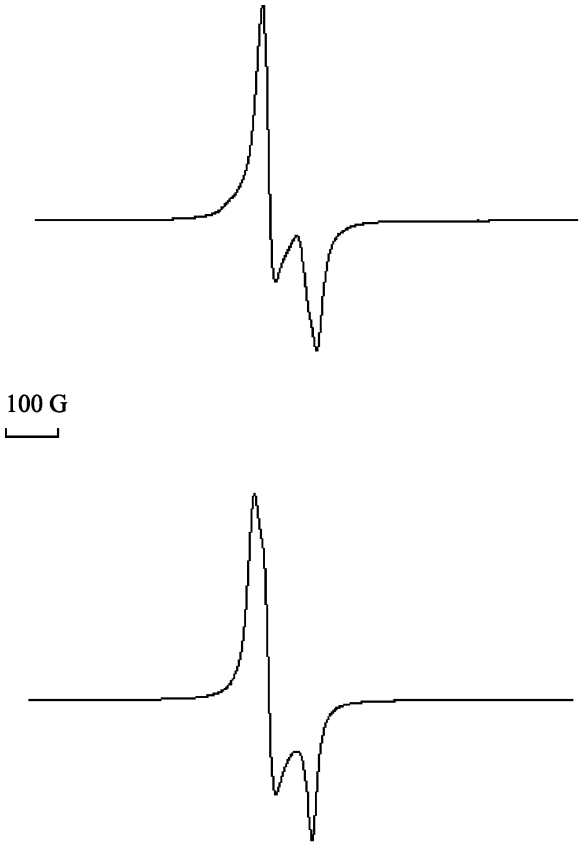

Fig. 4. ESR spectra of **1** (top) and **2** (bottom) at room temperature.

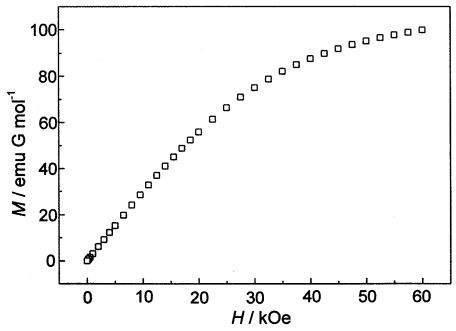

Fig. 5. M–H curve of **1** measured at 1.8 K.

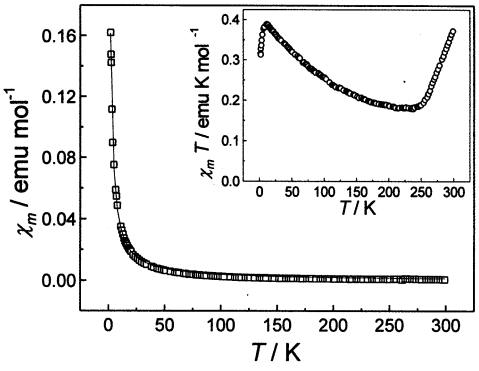

Fig. 6. Variation of molar magnetic susceptibility χ_m of **2** as a function of temperature. The solid line represents the best fit (inset: $\chi_m T$ vs. T plot).

and $g = 2.10$. As for **2**, the g-tensors are $g_x = 2.104$, $g_y = 2.091$, $g_z = 2.042$, respectively (cf. bottom of Fig. 4). Additionally, the field dependence of the magnetization (0–60 kOe) measured at 1.8 K shows the highest magnetization reaching a value of approximately 91 emu G mol^{-1} at 60 kOe, which is also significantly smaller than the expected value for a $S = 1/2$, $g = 2$ system (when Ni(III) is in a low spin state).

3.3. Electrochemistry

The cyclic voltammograms of **1** and **2** display two quasi-reversible one-electron redox processes. As an example, Fig. 7 shows the CV curve of [FBzPy][Ni(bdt)$_2$] (**1**), and the half-wave potentials versus Ag/AgCl are 379 mV [$\Delta E = 112$ mV] and −497 mV [$\Delta E = 99$ mV], respectively. The former wave is assigned to the redox couple of $[Ni(bdt)_2]^{1-/0}$, and the later one to the redox couple of $[Ni(bdt)_2]^{1-/2-}$. For **2**, the corresponding half-wave potentials versus Ag/AgCl are 353 mV [$\Delta E =$ 107 mV] and −472 mV [$\Delta E = 103$ mV], respectively. The redox potentials of the [Ni(bdt)$_2$] couples of two complexes lie in the same range as observed for other planar nickel complexes with four sulfur donors [6b,6c].

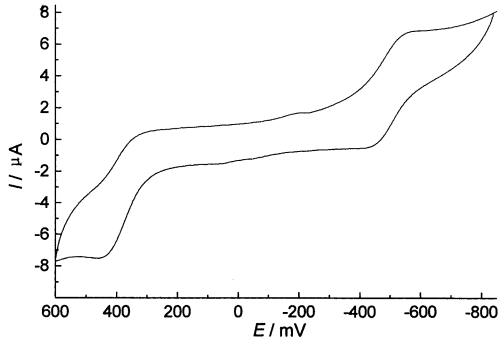

Fig. 7. Cyclic voltammogram of [FBzPy][Ni(bdt)$_2$] (**1**) in CH_3CN.

4. Conclusion

In this contribution, we fabricated two new ion-pair complexes containing the $[Ni(bdt)_2]^-$ unit. Two non-equiv. anions are stacked in different fashion, i.e. face to face or side by side in the two complexes. To our best knowledge, this structural motif is unprecedented in the chemistry of $[M(bdt)_2]^-$ complexes and is remarkably different from the corresponding $[M(mnt)]^-$ complexes. The magnetic properties of two complexes show that the primary exchange process involves antiferromagnetic coupling between nickel centers with a canting of the spins, that is to say, the weak ferromagnetism of **1** and **2** at low temperature may be due to a consequence of canted spin antiferromagnetism.

5. Supplementary material

Crystallographic data for the structural analysis have been deposited at the Cambridge Crystallographic Data Center, CCDC No. 177862 for complex **1**, 188273 for complex **2**. Copies of this information can be obtained free of charge on application to CCDC, 12 Union Road, Cambridge CB2 1EZ, UK (fax: +44-1223-336033; e-mail: deposit@ccdc.cam.ac.uk. or www: http://www.ccdc.cam.ac.uk).

Acknowledgements

The authors thank the National Natural Science Foundation, the State Education Commission of China and the State Key Laboratory of Structural Chemistry for financial support.

References

[1] R.-M. Olk, B. Olk, W. Dietzsch, R. Kirmse, E. Hoyer, Coord. Chem. Rev. 117 (1992) 99 (and references therein).
[2] (a) N.J. Long, Angew. Chem., Int. Ed. Engl. 34 (1995) 21; (b) C.S. Winter, S.N. Oliver, J.D. Rush, R.J. Manning, C. Hill, A.

Underhill, ACS Symp. Ser. 455 (1991) 616;
(c) T. Bjornholm, T. Geisler, J.C. Petersen, D.R. Greve, N.C. Schiodt, Non. Linear Optics 10 (1995) 129.
[3] (a) D. Sellmann, H. Friedrich, F. Knoch, M. Moll, Z. Naturforsch., Teil. B 48 (1994) 76;
(b) D. Sellmann, M. Waeber, Z. Naturforsch., Teil. B 41 (1986) 877;
(c) D. Sellmann, E. Böhlen, M. Waeber, G. Huttner, L. Zsolnai, Angew. Chem. 97 (1985) 984;
(d) D. Sellmann, E. Böhlen, M. Waeber, G. Huttner, L. Zsolnai, Angew. Chem., Int. Ed. Engl. 24 (1985) 981.
[4] (a) D. Sellmann, W. Soglowek, F. Knoch, M. Moll, Angew. Chem., Int. Ed. Engl. 28 (1989) 1271;
(b) D. Sellmann, W. Soglowek, F. Knoch, Inorg. Chem. 31 (1992) 3711;
(c) D. Sellmann, S. Fünfgelder, G. Pöhlmann, F. Knoch, M. Moll, Inorg. Chem. 29 (1990) 4772.
[5] (a) M.J. Baker-Hawkes, E. Billig, H.B. Gray, J. Am. Chem. Soc. 88 (1966) 4870;
(b) D. Sellmann, A.C. Hennige, F.W. Heinemann, Eur. J. Inorg. Chem. (1998) 819.;
(c) B.S. Kang, L.H. Weng, D.X. Wu, F. Wang, Z. Guo, L.R. Huang, Z.Y. Huang, H.Q. Liu, Inorg. Chem. 27 (1988) 1128.
[6] (a) C. Mahadevan, M. Seshasayee, P. Kuppusamy, J. Crystallogr. Spectrosc. Res. 15/4 (1985) 305;
(b) D. Sellmann, S. Fünfgelder, F. Knoch, M. Moll, Z. Naturforsch., Teil. B 46 (1991) 1601;
(c) D. Sellmann, H. Binder, D. Häußinger, F.W. Heinemann, J. Sutter, Inorg. Chim. Acta 300–302 (2000) 829.
[7] (a) X.M. Ren, C.S. Lu, Y.J. Liu, H.Z. Zhu, H.F. Li, C.J. Hu, Q.J. Meng, Transition Met. Chem. 26 (2001) 136;
(b) X.M. Ren, H.F. Li, P.H. Wu, Q.J. Meng, Acta Crystallogr., Sect. C C57 (2001) 1022;
(c) X.H. Zhu, X.Z. You, X.M. Ren, W.L. Tan, W. Dai, S.S.S. Raj, H.K. Fun, Chem. Lett. (2000) 472.
[8] S.B. Bulgarevich, D.V. Bren, D.Y. Movshovic, J. Mol. Struct. 317 (1994) 147.
[9] G.M. Sheldrick, In: SHELXTL, Structure Determination Software Programs, Version 5.10, 1992.
[10] U. Herzog, U. Böhme, G. Rheinwald, J. Organomet. Chem. 612 (2000) 133.
[11] (a) A. Davison, N. Edelstein, R.H. Holm, A.H. Maki, Inorg. Chem. 3 (1964) 814;
(b) A. Davison, N. Edelstein, R.H. Holm, A.H. Maki, J. Am. Chem. Soc. 85 (1963) 2029.
[12] (a) R.L. Carling, Magnetochemistry, Springer, Berlin, 1986;
(b) A.J. Banister, N. Bricklebank, I. Lavender, J.M. Rawson, C.I. Gregory, B.K. Tanner, W. Clegg, M.R.J. Elsegood, F. Palacio, Angew. Chem., Int. Ed. Engl. 35 (1996) 2533;
(c) N. Robertson, C. Bergemann, H. Becker, P. Agarwal, S.R. Julian, R.H. Friend, N.J. Hatton, A.E. Underhill, A. Kobayashi, J. Mater. Chem. 9 (1999) 1713.
[13] C.M. Liu, Z. Yu, R.G. Xiong, K. Liu, X.Z. You, Inorg. Chem. Commun. 2 (1999) 31.
[14] J.C. Bonner, M.E. Fisher, Phys. Rev. A 135 (1964) 640.
[15] W.E. Estes, D.P. Gavel, W.E. Hatfield, D.J. Hodgson, Inorg. Chem. 17 (1978) 1415.